World Academy of Science, Engineering and Technology
International Journal of Mechanical and Mechatronics Engineering
Vol:4, No:9, 2010

Visual Study on Flow Patterns and Heat Transfer during Convective Boiling Inside Horizontal Smooth and Microfin Tubes

V.D. Hatamipour, M.A. Akhavan-Behabadi

Digital Open Science Index, Mechanical and Mechatronics Engineering Vol:4, No:9, 2010 waset.org/Publication/9289

***Abstract*—**Evaporator is an important and widely used heat exchanger in air conditioning and refrigeration industries. Different methods have been used by investigators to increase the heat transfer rates in evaporators. One of the passive techniques to enhance heat transfer coefficient is the application of microfin tubes. The mechanism of heat transfer augmentation in microfin tubes is dependent on the flow regime of two-phase flow. Therefore many investigations of the flow patterns for in-tube evaporation have been reported in literatures. The gravitational force, surface tension and the vapor-liquid interfacial shear stress are known as three dominant factors controlling the vapor and liquid distribution inside the tube. A review of the existing literature reveals that the previous investigations were concerned with the two-phase flow pattern for flow boiling in horizontal tubes [12], [9]. Therefore, the objective of the present investigation is to obtain information about the two-phase flow patterns for evaporation of R-134a inside horizontal smooth and microfin tubes. Also Investigation of heat transfer during flow boiling of R-134a inside horizontal microfin and smooth tube have been carried out experimentally The heat transfer coefficients for annular flow in the smooth tube is shown to agree well with Gungor and Winterton's correlation [4]. All the flow patterns occurred in the test can be divided into three dominant regimes, i.e., stratified-wavy flow, wavy-annular flow and annular flow. Experimental data are plotted in two kinds of flow maps, i.e., Weber number for the vapor versus weber number for the liquid flow map and mass flux versus vapor quality flow map. The transition from wavy-annular flow to annular or stratified-wavy flow is identified in the flow maps.

***Keywords*—**Flow boiling, Flow pattern, Heat transfer, Horizontal, Smooth tube, Microfin tube.

I. Introduction

HEAT exchangers in air conditioning and heat pump applications play an important role on system efficiency and physical size. Therefore, the design of an efficient heat exchanger, especially evaporators and condensers, has always been significant to equipment designers and several enhancement techniques, e.g., twisted-tape inserts, corrugated tubes and microfin tubes, have been tested [3], [6], [8]. These techniques can be broadly classified into two main categories, viz., active techniques and passive techniques [7]. Active techniques require external energy to enhance heat transfer; however, passive techniques are such one, which need no external power for heat transfer enhancement. One of these passive techniques is the use of microfin tubes. Because of importance of microfin tubes in present work we experimentally investigated microfin tubes.

On the cases of in tube convective boiling, accurate modeling and trustworthy evaluation of heat transfer and pressure drop characteristics require precise predictions of the local two-phase flow patterns, the heat transfer coefficient generally keeps changing as the flow pattern changes along an evaporator tube [5]. since distinct flow regimes can be characterized by quite different flow and heat transfer mechanisms. Therefore, studies of two-phase flow patterns and their transitions during in tube flow boiling have gained increasing interest for several decades. Ref. [9] proposed a diabatic flow pattern map for evaporation (boiling) in horizontal straight smooth tube. They stated that their flow pattern map was developed based on flow pattern data for five different refrigerants, including R134a. Ref. [10] investigated the flow patterns in flow boiling and convective condensation of refrigerant R22 in a microfin tube.

The flow patterns could be characterized as a function of mass flow rate, vapor quality and fluid properties.

Baker (1954) classified the two-phase flow pattern of air–water mixture in tubes of small diameters (<0.05 m) by using the mass velocity. Ref. [1] used flow rate and exit quality to plot the flow pattern maps. So the objective of the present investigation is to obtain information about the two-phase flow patterns for evaporation of R-134a inside horizontal smooth and microfin tubes.

II. Nomenclature

A	tube inside cross-sectional area (m^2)
j	superficial velocity ($m.s^{-1}$)
D	Tube diameter (m)
D_o	outside diameter of test-section(m)
G	mass velocity ($kg.s^{-1}.m^{-2}$)
M	mass fow rate ($kg.s^{-1}$)
Q	heat transfer rate (W)
T	temperature (K)
T_s	average saturation temperature of refrigerant (K)

V.D. Hatamipour is with the Department of Mechanical Engineering, Tehran University (Phone: + (98)-21-88337123, Fax: + (98)-21-88337123 e-mail: v.hatami@ ut.ac.ir).

Prof. M.A. Akhavan-Behabadi, is with the Department of Mechanical Engineering, Tehran University (email address: akhavan@ut.ac.ir).

Digital Open Science Index, Mechanical and Mechatronics Engineering Vol:4, No:9, 2010 waset.org/Publication/9289

T_{wi}	average inside test-section wall temperature (*K*)
T_{wo}	average outside test-section wall temperature (*K*)
We	Weber number
x	vapor quality
h	heat transfer coefficient ($W\ m^{-2}\ K^{-1}$)
L	length of test-section (*m*)
Greek letters	
ρ	density ($kg.\ m^{-3}$)
σ	surface tension($N.\ m^{-1}$)
Subsripts	
g	vapor phase
l	liquid phase

III. Experimental Facility

The experimental set-up was a well instrumented vapor compression refrigeration system. The schematic diagram of experimental set-up is shown in fig 1.

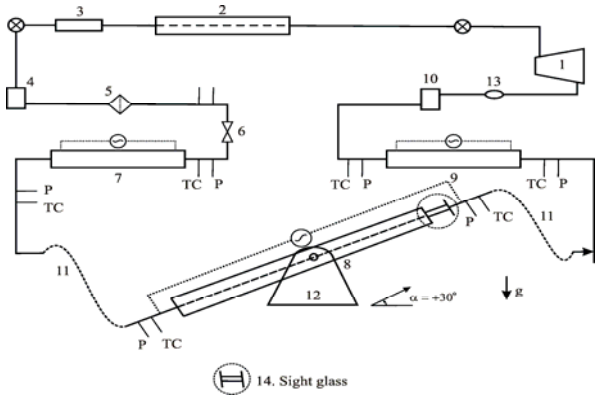

1- COMPRESSOR	11- FLEXIBLE HOSE(for R134a)
2- CONDENSER	12- ROTATING TRESTLE
3- ROTAMETER	13- SIGHT GLASS
4- RECIEVER	TC- THERMOCOUPLE
5- FILTER DRIER	P- PRESSURE GUAGE
6- EXPANSION VALVE	T- THRMOMETER
7- PRE-EVAPORATOR	SHUT OFF VALVE
8- TEST-EVAPORATOR	WATER FLOW
9- AFTER-EVAPORATOR	REFRIGERANT FLOW
10- ACCUMULATOR	ELECTRICAL POWER SUPPLY

Fig. 1 Schematic diagram of experimental set-up

The set-up included a test- evaporator, a pre-evaporator, and an after-evaporator. These tubes were heated by flexible electrical heating tapes of 2kW capacity, wrapped around them.

In order to change the inclination angle of the test-evaporator the connections to this evaporator were made by special flexible pressure hoses for R-134a. In order to cover the whole domain of vapor quality, a pre-evaporator was used. The fluid emerging from test-evaporator was passed through the after-evaporator for the complete evaporation of R-134a liquid. The electrical power of heater in each three evaporators was regulated in order to control the quality of refrigerant vapor entering the test evaporator. Then the refrigerant vapor was circulated inside the condenser with the help of a reciprocating compressor.

The condensed R-134a enters the rotameter, expands in expansion valve and enters the pre-evaporator again. The test section is a 1.1 m long horizontal mounted copper tube. Two tubes were tested in the study. A microfin tube with 9.52 OD, 55 fins, and 15˚ helix angle and the nominal inside diameter of the microfin tube is 8.92 mm with ridge height of 0.25 mm, and a smooth tube with same inside tube diameter. The microfin tube was a copper tube having internal micro-fins with triangular fin cross-section. The geometrical parameters of microfin tube are shown in figure 2.

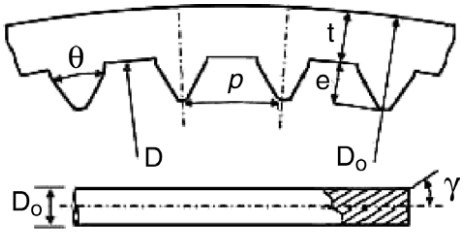

fin tip angle	θ	25°
helix angle	γ	15°
outside diameter	D_o	9.52 mm
inside diameter	D	8.92 mm
fin height	*e*	0.25 mm
wall thickness	t	0.30 mm
fin pitch	p	0.48mm
number of fins	n	55

Fig. 2 Dimensions of standard microfin tube

The two-phase flow patterns were observed visually and the transition locations between different flow patterns were measured in a transparent test section. A pyrex glass window is mounted at end of test section for flow pattern visualization. The sight glass has a length of 100 mm and an inner diameter identical to that of the test section. A digital camera is used to record flow patterns in the sight glass. At the same time in test procedure, naked eye observations are also written down for references.

The inner diameter of the sight glass is equal to that of both test tubes and the connections. A camera based flow visualization technique was used in this study is shown in figure 3. A canon camera with adjustable focal length and shutter speed is used to capture the images. Best images were captured in 8000 fps shutter speed.

A diffuse white film pigmented with evenly spaced black stripes are placed in the background (behind the glass tube) and illuminated with a stroboscope directed towards the camera. The stripe width, spacing, and distance from the centerline of the test sections are presented by Jassim (2006).

At the same time in test procedure, naked eye observations

Digital Open Science Index, Mechanical and Mechatronics Engineering Vol:4, No:9, 2010 waset.org/Publication/9289

are also written down for references. It is noteworthy to point out that flow patterns are observed through sight glasses which are not microfin, but nevertheless they are assumed as fully representatives of the flow regimes actually occurring at the test section exit. Indeed, Wenzhi Cui et al. (2007) conjectured that the flow structure should experience only a minor disruption in passing to the glass tube, and the flow should not redevelop through the sight glass because of its short length.

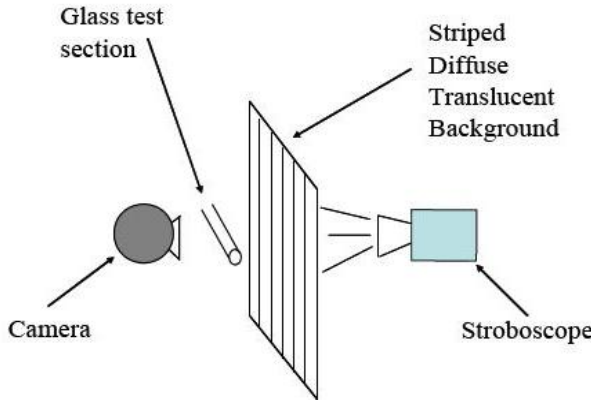

Fig. 3 Flow visualization schematic

IV. Measurements

The average outside wall temperatures of the tube was measured at six axial locations. At each location four thermocouples were fixed at top, two sides and bottom positions (when microfin tube is in horizontal position). The refrigerant temperatures at the inlet and outlet of the test-evaporator were also measured. All the above temperature measurements were done by T type (Cu-Constantan) thermocouples with a calibrated accuracy of 0.1 °C. The thermocouples were carefully soldered on the outer surface of microfin tube at six sections with each 20 cm distance along the tube. The arrangements were also made for the measurement of refrigerant pressure at inlet and outlet of the test-evaporator, pre-evaporator and after-evaporator. The refrigerant mass flow rate was measured by a rotameter installed down stream of condenser.

It was ensured that the refrigerant enters the rotameter was completely liquid, whenever it was not seen any bubble in the condensed refrigerant liquid. The whole of test-evaporator, pre-evaporator and after-evaporator were insulated by glass wool and AFLEX tube insulations to prevent any heat loss to the surroundings.

A total of 80 test runs with four different refrigerant mass velocities of 53.66, 78.32, 107.26 and 153.74 $kg.m^{-2}.s^{-1}$ were performed for horizonal smooth tube and four refrigerant mass velocities of 58.3, 74.46, 97.54 and 157.17 $kg.m^{-2}.s^{-1}$ were performed for horizontal microfin tube. The range of operating parameters is given in table 1.

TABLE I
THE RANGES OF OPERATING PARAMETERS

Working fluid :	R-134a
Refrigerant mass velocity :	56 to 157 $kg/m^2.s$
Average evaporating temperature:	-24.4 to -5.1 °C
Average heat flux:	2.2 to 6.2 kw/m^2
Average vapor quality:	0.1 to 0.96

The vapor quality at the inlet of pre-evaporator was computed by considering the isoenthalpic expansion of refrigerant in the needle valve. An energy balance technique was used to get the vapor quality of the inlet and the exit of test-evaporator. The mean vapor quality was taken as the average of inlet and outlet vapor qualities of test-section. The heat transfer coefficient of test-section was determined using the heat gain from electrical heater and the temperature difference between the evaporator inside wall surface and the boiling refrigerant.

The average outside tube wall temperature of test-evaporator at a particular station, T_{wo}, was calculated by using Equation 1.

$$T_{wo} = \frac{T_t + 2T_s + T_b}{4} \quad (1)$$

The average outside tube wall temperature of test-evaporator, T_{wo}, was computed by taking the average temperatures of six axial stations as:

$$\overline{T}_{wo} = \frac{\sum_{1}^{6} T_{wo}}{6} \quad (2)$$

The radial heat flux, q , for test-evaporator was calculated by Equation 3.

$$q = Q/(\pi DL) \quad (3)$$

Temperature inside the tube wall, ΔT_{wi}, was determined using Equation 4 for radial heat flux.

$$\Delta T_{wi} = \frac{q d_i \ln(d_o/d_i)}{2k_w} \quad (4)$$

The average static pressure in test-evaporator was taken to be the mean of the inlet and outlet pressure. The vapor saturation temperature in test-evaporator, T_s, was taken as the saturation temperature corresponding to this average static pressure. The heat transfer coefficient of test-evaporator was calculated by the following Equation 5.

$$h = \frac{q}{(T_{wi} - T_s)} \quad (5)$$

The thermo-physical properties of R-134a were taken from [11], [13]. The uncertainty analysis of experimental results has

Digital Open Science Index, Mechanical and Mechatronics Engineering Vol:4, No:9, 2010 waset.org/Publication/9289

been carried out by the method proposed in [2]. It was found that the expected experimental uncertainty was within a band of ±9.33% for all the test runs.

V. Results and Discussion

A. Flow Pattern

In the test, all the flow patterns observed in the horizontal microfin and smooth tubes can be classified into stratified-wavy flow, wavy-annular flow and annular flow. Fig. 4 shows the photographs of three main flow patterns captured by digital camera.

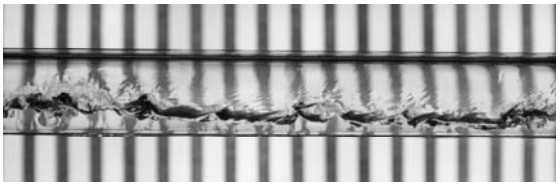

(a) stratified-wavy flow

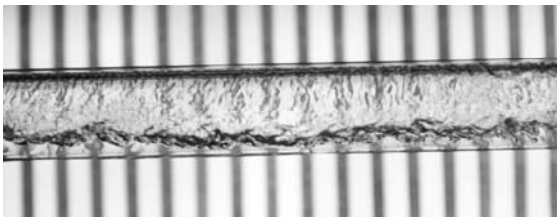

(b) Wavy-annular Flow

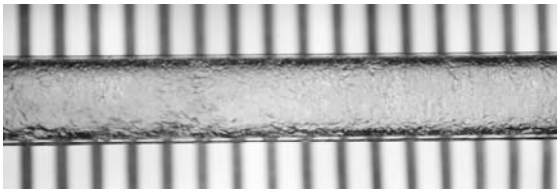

(c) Annular Flow

Fig. 4 Flow patterns in horizontal microfin and plain tube

The structure of stratified-wavy flow pattern is shown in fig. 4(a). This flow pattern is characterized by a complete gravitational separation of the liquid and vapor phases by a wavy interface. The liquid flows along the bottom and vapor flows over it along the top of the tube. Due to the velocity difference between the two phases, the liquid–vapor interface is disturbed by the vapor stream and becomes wavy.

This flow pattern is similar to annular flow except that the liquid layer at the bottom of the tube is much thicker than that at the top. The vapor–liquid interface is wavy due to disturbance by the high-speed vapor stream. Wavy-annular is shown in fig. 4(b).

In almost high vapor quality flows, the interfacial shear of the high velocity gas on the liquid film becomes dominant over gravity, so the liquid is expelled from the center of the tube and flows as a thin film on the wall while the gas flows as a continuous phase up the center of the tube..This flow pattern is characterized by complete separation of the liquid and vapor phases, with flowing of the liquid film on the tube wall and vapor in the tube core. The entire circumference of the tube wall is continuously wetted by a liquid film of nonuniform thickness. Some of the small droplets may be entrained in the vapor core. Annular flow regime which is shown in fig. 4(c), is particularly stable [14].

Flow pattern maps are often used to depict the transitions of different flow patterns, although different flow characteristics exist between two-phase flow in the straight tube. Fig. 5 shows the flow pattern map for the present flow boiling in microfin tube. In Fig. 5, the abscissa and ordinate are Weber number for the liquid and weber number for the vapor, respectively.

The refrigerant mass velocity in the tube is defined as:

$$G = \frac{m}{A} \tag{6}$$

The superficial liquid velocity and the superficial vapor velocity are

$$J_L = \frac{G(1-x)}{\rho_L} \tag{7}$$

$$J_G = \frac{Gx}{\rho_G} \tag{8}$$

The corresponding Weber numbers are defined respectively as:

$$We_L = \frac{J_L^2 D \rho_L}{\sigma} \tag{9}$$

$$We_G = \frac{J_G^2 D \rho_G}{\sigma} \tag{10}$$

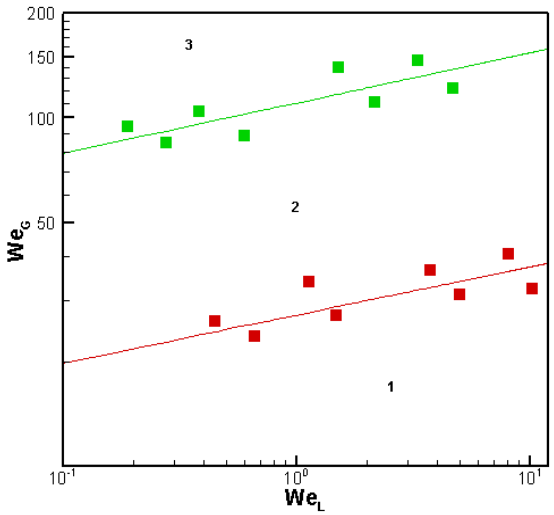

1-Churn Flow; 2-Wavy Annular Flow; 3-Annular Flow

Fig. 5 $We_G - We_L$ flow pattern map for horizontal microfin tube

Digital Open Science Index, Mechanical and Mechatronics Engineering Vol:4, No:9, 2010 waset.org/Publication/9289

to better identify flow patterns during the evaporation process at different mass velocities and to make the map a more useful research and design tool, the axes of the previous flow pattern map have been converted to mass flux versus vapor quality (similar to how local flow boiling coefficients are plotted, i.e., heat transfer coefficient versus vapor quality) Fig. 6 shows such kind of flow map.

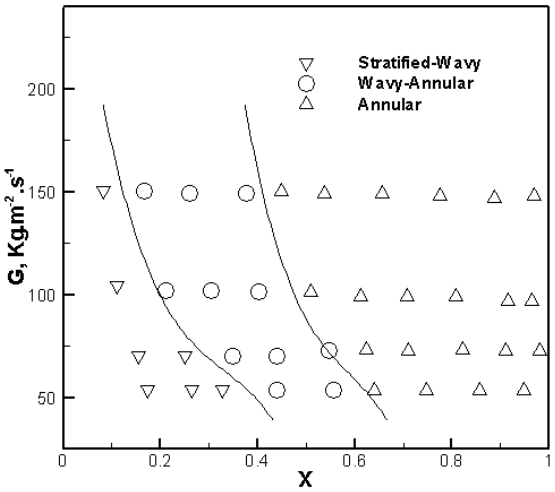

Fig. 6 $G-x$ flow pattern map for horizontal microfin tube

According to Fig. 6 transition between stratified wavy flow and wavy annular flow is at $x=0.2$. And flow pattern remain wavy annular till almost $x=0.45$. After that in all mass flow velocities for vapour qualities greater than $x=0.45$ flow pattern is annular flow.

Also in this experiment flow patterns of horizontal plain tube are observed. In almost same conditions as horizontal flow in microfin tube flow maps are plotted. There are two kinds of flow maps for horizontal flow in smooth tube, Weber number for the vapor versus weber number for the liquid flow map and mass flux versus vapor quality flow map. Fig. 7 shows Weber number for the vapor versus weber number for the liquid flow map in horizontal smooth tube.

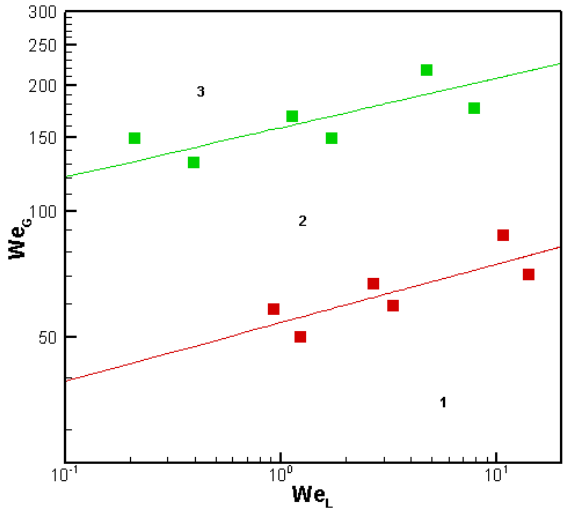

1-Churn Flow; 2-Wavy Annular Flow; 3-Annular Flow

Fig. 7 $We_G - We_L$ flow pattern map for horizontal smooth tube

Fig. 8 shows mass flux versus vapour quality flow map for horizontal smooth tube.

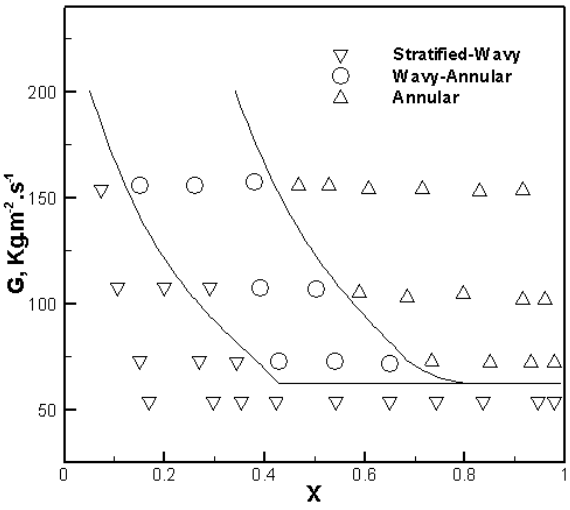

Fig. 8 $G-x$ flow pattern map for horizontal smooth tube

VI. Heat Transfer Coefficient

The calculated experimental heat transfer coefficients of the present horizontal flow in smooth tube were compared with the three existing correlations of Gungor and Winterton [10], Koyama et al. [6], and Wellsandt and Vamling [11]. It was concluded that Gungor and Winterton [10], correlation predicts the experimental microfin tube horizontal flow data within an error band of -14.1% to +21.3% . The estimation of the correlation of Koyama et al. was within -33.8% to +19.4% of the experimental horizontal flow values.

Digital Open Science Index, Mechanical and Mechatronics Engineering Vol:4, No:9, 2010 waset.org/Publication/9289

This agreement of experimental heat transfer coefficients of horizontal flows with the predicted values establishes the integrity of experimental set-up.

The variation of evaporation heat transfer coefficient, h, with vapor quality of microfin and smooth tube have been drawn in figures 9-10 for four mass velocities of R-134a form 53.66 to 157.17 kg/m^2.s.

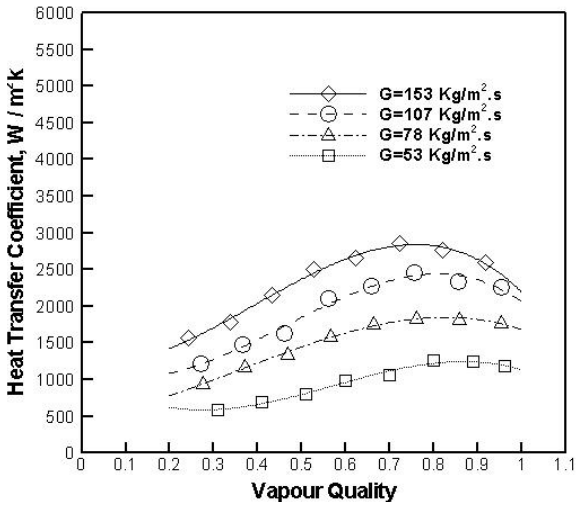

Fig. 9. Variation of heat transfer coefficient with mass velocity in horizontal flow smooth tube

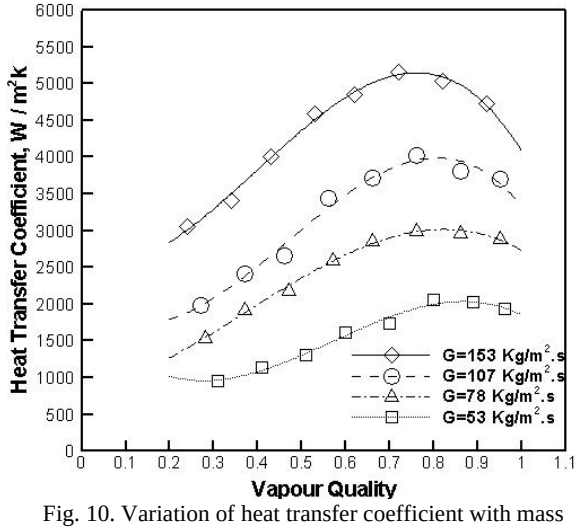

Fig. 10. Variation of heat transfer coefficient with mass velocity in horizontal flow microfin tube

It is observed from Figures 9-10, that the heat transfer coefficient increases with the increase of flow mass velocity for smooth and microfin tubes. Also it is noted that the increase of heat transfer coefficient for both tubes is occurred in the same way.

The heat transfer coefficient increases with the increase of vapor quality up to a maximum value and then it decreases with more increases in vapor quality. The reason for such a phenomenon is the fact that, as the vapor quality increases the thickness of annular liquid film inside the tube decreases and subsequently decreases liquid film thickness offers lower thermal resistance of liquid film to heat flow from electrical heater to the vapor side of liquid film surface. Furthermore, as the evaporation progresses, the vapor phase velocity increases resulting in the raising of the interfacial shear stresses. The cumulative effect of the above two factors contributes towards the increase in the heat transfer coefficient, h. Finally after a maximum value, there is often a reduction in heat transfer coefficient due to the tube circumference is only partially wetted with liquid.

Horizontal microfin tube increases the heat transfer coefficient by 0.65 percent in comparison to that for the horizontal smooth tube at high vapour quality region at the mass velocities of 100 and 150 kg/m^2.s.

VII. Conclusions

Two-phase flow regimes and heat transfer coefficient of refrigerant R134a boiling in microfin and smooth tube are experimentally studied in this paper. The flow patterns are identified using visualization methods and grouped into three dominant regimes, i.e., stratified-wavy flow, wavy-annular flow and annular flow. Flow map is used to figure out the transitions of different flow patterns. Two kinds of usually used flow maps, i.e., Weber number for the vapor versus weber number for the liquid ($We_G - We_L$) flow map and mass flux versus vapor quality ($G - x$) flow map, are chosen in this study.

At high vapor quality region annular flow is observed and in low vapor qualities stratified-wavy flow is captured. And in a small region between two previous regions wavy annular flow is observed.

It was found microfin tube have a noticeable effect on heat transfer coefficient. Horizontal microfin tube increases the heat transfer coefficient by 0.65 percent in comparison to that for the horizontal smooth tube at high vapour quality region at the mass velocities of 100 and 150 kg/m^2.s.

It was revealed heat transfer coefficient increases with the increase of flow mass velocity for smooth and microfin tubes.

References

[1] Bergles, AE & Suo, M. Investigation of boiling water flow regimes at high pressure. In: Proc. Heat Trans. Fluid Mech. Institute. Stanford Press, p. 77–79 (1966)

[2] Schultz, R.R. & Cole, R. Uncertainty Analysis in Boiling Nucleation, *AIChE Symp. Series*, Vol.75, No.189, pp. 32-38, (1979)

[3] Agrawal, K.N. & Varma, H.K. & Lal, S.N. Heat Transfer During Forced Convection Boiling of R12 Under Swirl Flow, *ASME J. Heat Transfer*, Vol. 108, pp. 567–573, (1986)

[4] Gungor, K.E. & Winterton, R.H. Simplified General Correlation for Saturated Flow Boiling and Comparison of Correlations to Data", *Industrial & Engineering Chemistry Process Design and Developmen*t, Vol. 65, pp.148-156, (1987)

[5] Carey VP. Liquid-vapor phase-change phenomena. Washington (DC): Hemisphere Pub. Co, (1992)

[6] Thors, P. & Bogart, J.E. In-Tube Evaporation of HCFC-22 with Enhanced Tubes, *J. Enhanced Heat Transfer*, Vol. 1, pp. 365–

377, (1994)

[7] Webb, R.L. *Principles of Enhanced Heat Transfer*, John Wiley and Sons, New York (1994)

[8] Chamra, L. & Webb, R. & Randlett, M. Advanced Microfin Tubes for Evaporation, *International Journal of Heat and Mass Transfer*, Vol. 39 (9), pp.1827–1838, (1996)

[9] Kattan, N. & Thome, J.R. & Favrat, D. Flow boiling in horizontal tubes: Part 1: development of a diabatic two-phase flow pattern map. Journal of Heat Transfer ;120:140–7.(1998)

[10] Muzzio, A. & Niro, A. & Garavaglia, M. Flow patterns and heat transfer coefficients in flow-boiling and convective condensation of R22 inside a microfin tube of new design, in: Heat Transfer 1998, Proceedings of 11th IHTC, Kyongju, Korea, vol. 2, , pp. 291–296 (1998)

[11] Stoecker, W.F. *Industrial refrigeration handbook*, Mc Graw Hill Companies, Inc. (1998)

[12] Ming-huei, Yu. & Tsun-kuo, Lin & Chyuan-chyi, Tseng Heat transfer and flow pattern during two-phase flow boiling of R-134a in horizontal smooth and microfin tubes. International jornal of refrigeration (2001)

[13] Sonntag, R.E. & Borgnakke, C. & Van Wylen, G.J. *Fundamentals of Thermodynamics*, John wiley and sons, New York, (2003)

[14] Thome, J.R. *Engineering Data BookIII*, by Wolverin tube, Inc. (2004-2006)

Digital Open Science Index, Mechanical and Mechatronics Engineering Vol:4, No:9, 2010 waset.org/Publication/9289